

ABMP $t\bar{t}$: updated ABMP16 PDFs with differential $t\bar{t}$ data

Sergey Alekhin¹, Maria Vittoria Garzelli¹, Sven-Olaf Moch¹, Sasha Zenaiev¹

¹ Universität Hamburg, II. Institut für Theoretische Physik

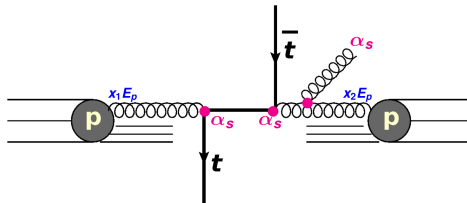
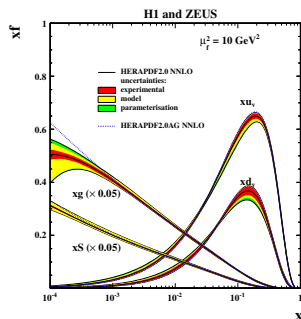
[Garzelli, Mazzitelli, Moch, Zenaiev JHEP 05 (2024) 321 [arXiv:2311.05509]]

[Alekhin, Garzelli, Moch, Zenaiev arXiv:2407.00545]

LHC EW WG General Meeting
11 Jul 2024

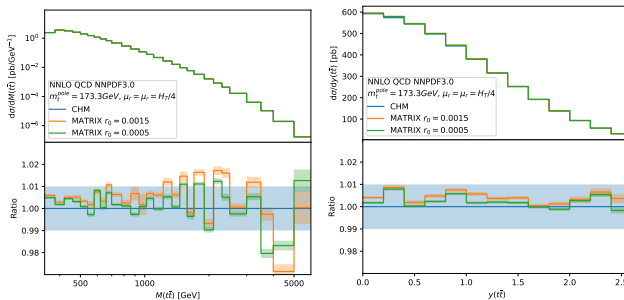
Importance of gluon PDF

- Parton distribution functions (PDFs) cannot be computed perturbatively and must be extracted from data: ep DIS, DY etc.
- In this work we focus on gluon PDF g : it is a challenge because is not directly constrained by DIS data (backbone of PDF fits)
 - especially at large x (important for BSM searches at LHC)
 - in addition, g is strongly correlated with α_S
- Processes to constrain g :
 - heavy-quark production: NNLO, but depend on m_Q
 - jet production: larger NNLO scale choice
- We focused on double-differential $t\bar{t}$ LHC data $d^2\sigma/M(t\bar{t})y(t\bar{t})$:
 - $M(t\bar{t})$ provides sensitivity to m_t
 - $y(t\bar{t})$ provides sensitivity to PDFs via relation to partonic momentum fraction x : $x_{1,2} = (M(t\bar{t})/\sqrt{s}) \exp [\pm y(t\bar{t})]$



Theoretical calculations and scope of our work

- NNLO calculations for total and fully differential $t\bar{t}$ (q_T subtraction) are publicly available with MATRIX framework Catani et al. PRD99 (2019) 5, 051501 Catani et al. JHEP 07 (2019) 100
 - ▶ fully differential NNLO calculations were also published in Czakon, Heymes, Mitov JHEP 04 (2017) 071 [CHM], but no public code available

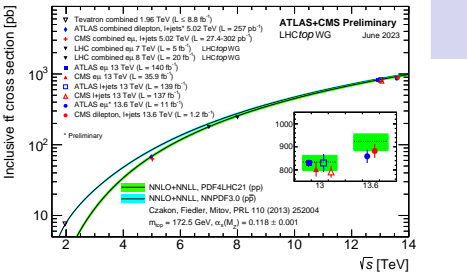


- We have interfaced MATRIX $t\bar{t}$ to PineAPPL interpolation library: **no NNLO/NLO K-factors**
- Garzelli, Mazzitelli, Moch, Zenaiev JHEP 05 (2024) 321: extraction of m_t^{pole} from the total and differential $t\bar{t}$ data using different PDF sets
- Alekhin, Garzelli, Moch, Zenaiev arXiv:2407.00545: **global PDF+ α_S+m_t fit within the ABMP16 framework**
 - ▶ using collider and fixed-target DIS, DY (see BACKUP), **updated single top and $t\bar{t}$ data**

Data used in this analysis

Selection of data:

- all LHC measurements of single t :
 - 6 data points from LHCTopWG
- all LHC measurements of total $\sigma(t\bar{t})$:
 - 10 data points, including recently combined CMS+ATLAS cross section at 7 and 8 TeV
- differential measurements $\frac{1}{\sigma(t\bar{t})} \frac{d\sigma(t\bar{t})}{dO}$ which satisfy following criteria:
 - as function of $M(t\bar{t})$ (if available, 2D $M(t\bar{t})$ and $y(t\bar{t})$)
 - unfolded to parton level (no cuts on p_T , y of leptons or jets): no LHCb data
 - bin-by-bin correlations are available (no Tevatron data)
 - normalized cross sections (to avoid unknown correlation with total $\sigma(t\bar{t})$ and to reduce unknown correlations between different data sets)
 - for the moment only Run-2 2D data included in the PDF fit (besides the total $t\bar{t}$ x-section data)



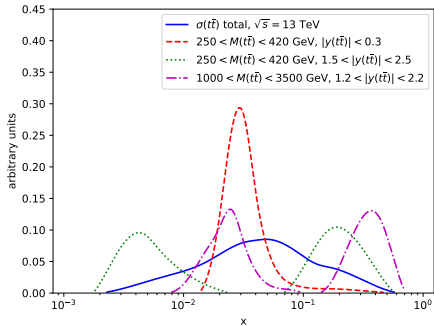
$$\frac{1}{\sigma(t\bar{t})} \frac{d\sigma(t\bar{t})}{dO}$$

Experiment	decay channel	dataset	luminosity	\sqrt{s}	observable(s)	n
CMS	semileptonic	2016–2018	137 fb $^{-1}$	13 TeV	$M(t\bar{t})$, $ y(t\bar{t}) $	34
CMS	dileptonic	2016	35.9 fb $^{-1}$	13 TeV	$M(t\bar{t})$, $ y(t\bar{t}) $	15
ATLAS	semileptonic	2015–2016	36 fb $^{-1}$	13 TeV	$M(t\bar{t})$, $ y(t\bar{t}) $	19
ATLAS	all-hadronic	2015–2016	36.1 fb $^{-1}$	13 TeV	$M(t\bar{t})$, $ y(t\bar{t}) $	10
CMS	dileptonic	2012	19.7 fb $^{-1}$	8 TeV	$M(t\bar{t})$, $ y(t\bar{t}) $	15
ATLAS	semileptonic	2012	20.3 fb $^{-1}$	8 TeV	$M(t\bar{t})$	6
ATLAS	dileptonic	2012	20.2 fb $^{-1}$	8 TeV	$M(t\bar{t})$	5
ATLAS	dileptonic	2011	4.6 fb $^{-1}$	7 TeV	$M(t\bar{t})$	4
ATLAS	semileptonic	2011	4.6 fb $^{-1}$	7 TeV	$M(t\bar{t})$	4

Kinematic region probed by $t\bar{t}$, DY and Higgs production

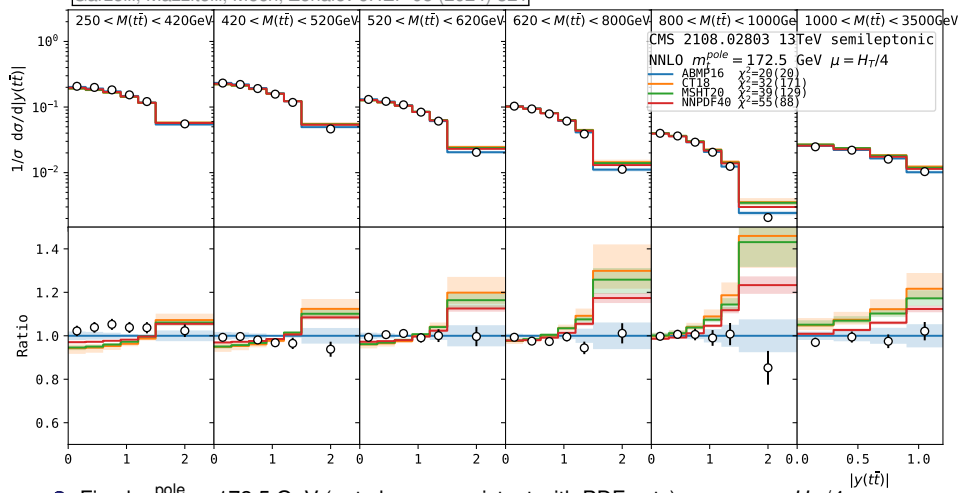
- Double-differential $t\bar{t}$ @ 13 TeV probes $0.002 \lesssim x \lesssim 0.7$
 - gg contributes $\approx 90\%$
- E.g. Higgs production at the LHC probes $x \sim m_H/\sqrt{s} \sim 0.01$ which is well covered by differential $t\bar{t}$ data
- Energy scales m_H, M_W, M_Z and m_t are similar
- DY production at the LHC probes a similar region $x \sim m_{W,Z}/\sqrt{s}$
 - sensitive to quark PDFs mostly
 - helps with light flavor separation
 - recent work [S. Alekhin et al., arXiv:2405.19714](#) confirmed NNLO used for DY in ABMP16 (in particular the issue of symmetric cuts): the effect of resummation is small beyond NNLO

$$\text{LO: } x_{1,2} = (M(t\bar{t})/\sqrt{s}) \exp [\pm y(t\bar{t})]$$



Example: CMS 2108.02803 vs NNLO predictions using different PDFs

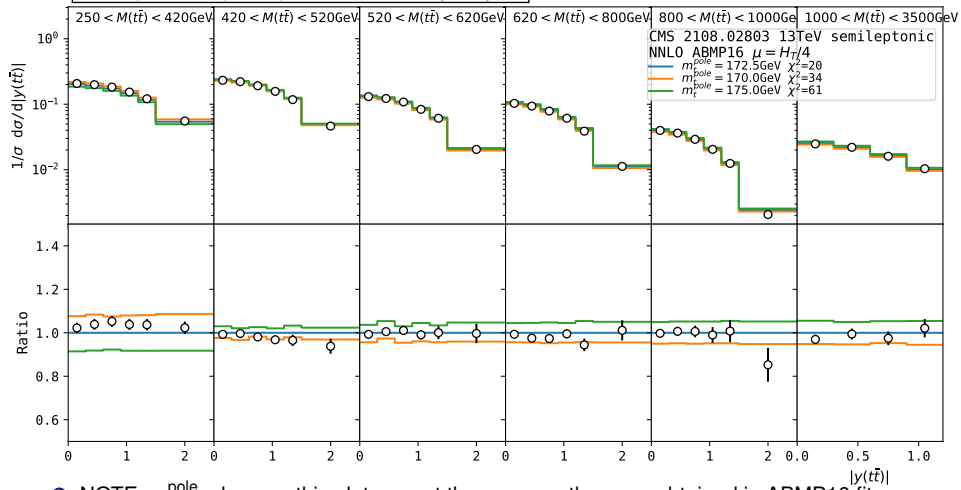
Garzelli, Mazzitelli, Moch, Zenaiev JHEP 05 (2024) 321



- Fixed $m_t^{\text{pole}} = 172.5 \text{ GeV}$ (not always consistent with PDF sets), $\mu_r = \mu_f = H_T/4$
- Reported χ^2 values with (and without) PDF uncertainties
- All PDF sets describe data reasonably well, with best description by ABMP16
 - ▶ CT18, MSHT20 and NNPDF40 show clear trend w.r.t data at high $y(t\bar{t})$ (large x)

Example: CMS 2108.02803 vs NNLO predictions using different m_t^{pole}

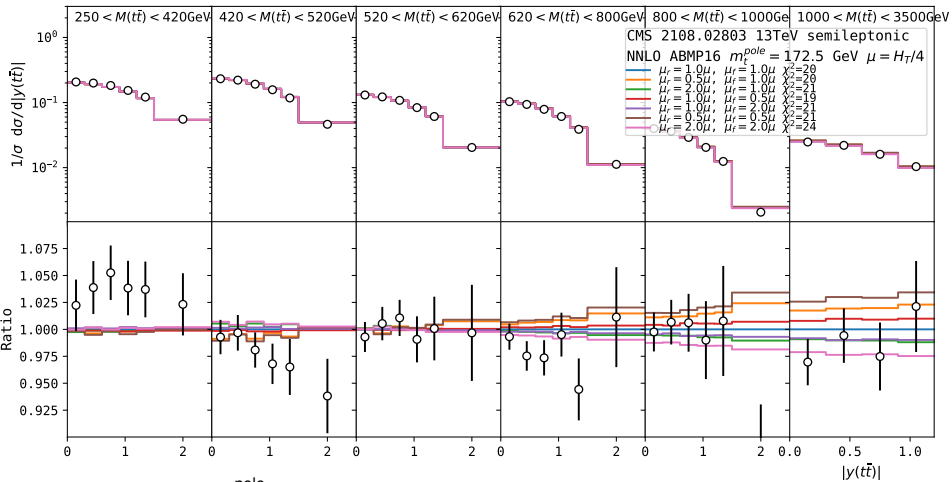
Garzelli, Mazzitelli, Moch, Zenaiev JHEP 05 (2024) 321



- NOTE: m_t^{pole} values on this plot are not the same as the ones obtained in ABMP16 fit ($m_t^{\text{pole}} = 170.4 \pm 1.2 \text{ GeV}$)
- Low $M(t\bar{t})$: strong dependence on m_t^{pole} via threshold effects
- High $M(t\bar{t})$: opposite dependence due to cross section normalization

Example: CMS 2108.02803 vs NNLO predictions: scale variations

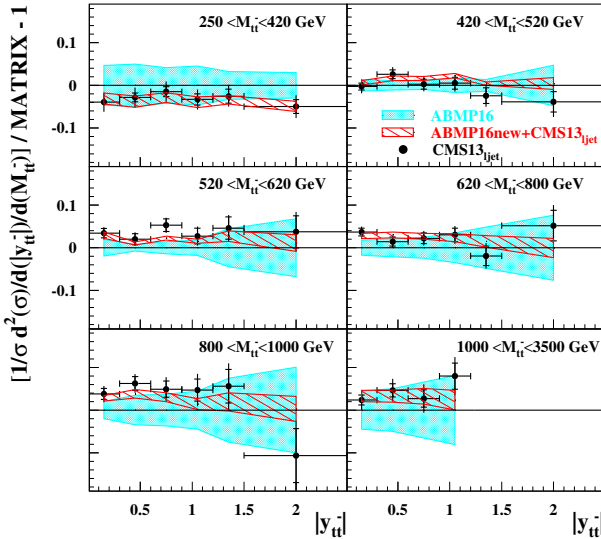
Garzelli, Mazzitelli, Moch, Zenaiev JHEP 05 (2024) 321



- ABMP16, fixed $m_t^{\text{pole}} = 172.5 \text{ GeV}$
- Scale variations $< 1\%$ at low $M(t\bar{t})$ (largest cancellation), reach $\approx 4\%$ at high $M(t\bar{t})$
- these data are useful to provide constraints on m_t and PDFs

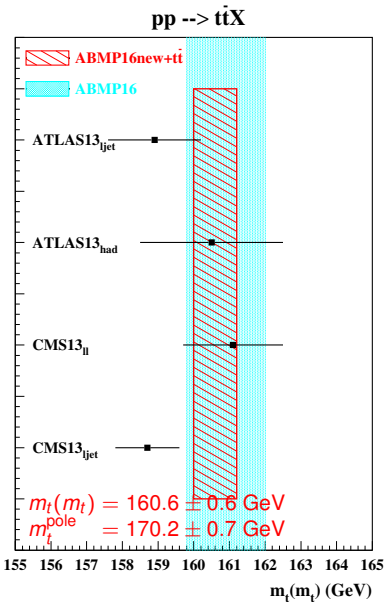
CMS 2108.02803 in ABMP16 PDF fit

CMS ($\sqrt{s}=13$ TeV, 137 fb^{-1} , pp $\rightarrow t\bar{t}X \rightarrow 1\text{jet}X$) 2108.02803

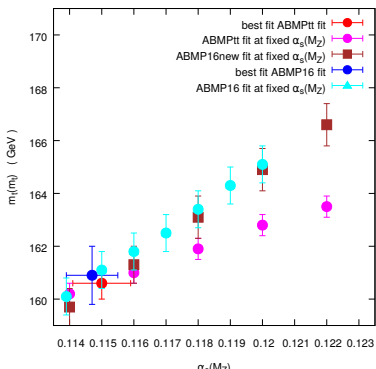


→ all data (including DY) are in good agreement with NNLO theoretical predictions and put significant constraints on the PDFs
 (other $t\bar{t}$ data sets in BACKUP)

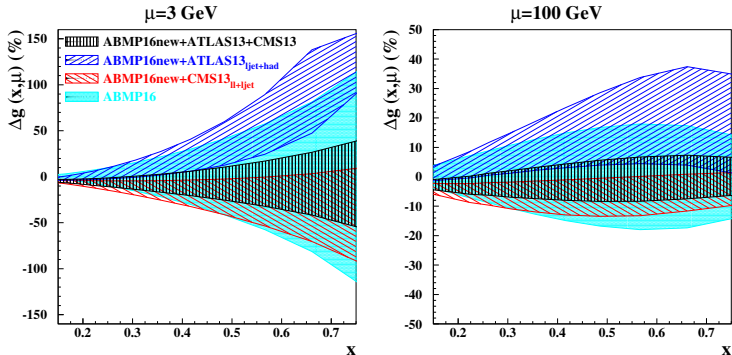
$m_t(m_t)$ and α_s in ABMP16 PDF fit



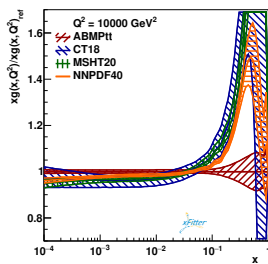
- Overall, good agreement between $m_t(m_t)$ extracted from different data sets
- Good agreement with ABMP16 fit and $\sim 50\%$ reduced uncertainty on $m_t(m_t)$
- ABMP16new: consistent with ABMP16, but with extra iteration for DY data
- Positive correlation between α_s and $m_t(m_t)$ reduced with $t\bar{t}$ differential data



Fitted gluon PDF



- Significant reduction of the gluon PDF uncertainty once differential $t\bar{t}$ data are included
- The fitted gluon PDF is consistent with ABMP16 and differs w.r.t to other global fits at large x
- Fitted $\alpha_S(M_Z) = 0.1150 \pm 0.0009$ in ABMPtt vs fixed $\alpha_S(M_Z) = 0.118$ in other fits
- we have confirmed ABMP16 gluon and α_S with new data (other distributions in BACKUP)



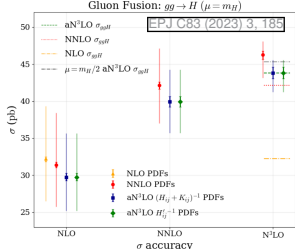
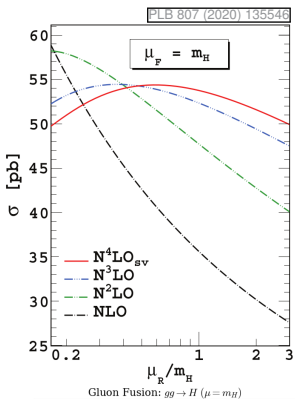
Higgs cross section with ABMPtt (contribution from Goutam Das)

PDF Name	N2LO	N3LO	N4LOsv
ABMP16	$(45.4 \pm 4.6)^{+0.7}_{-0.7}$	$(49.6 \pm 2.6)^{+0.8}_{-0.8}$	$(50.8 \pm 1.9)^{+0.9}_{-0.9}$
ABMPtt	$(45.0 \pm 4.6)^{+0.6}_{-0.6}$	$(49.2 \pm 2.6)^{+0.7}_{-0.7}$	$(50.4 \pm 1.9)^{+0.8}_{-0.8}$
CT18NNLO	$(47.4 \pm 5.1)^{+1.3}_{-1.7}$	$(52.0 \pm 2.9)^{+1.4}_{-1.9}$	$(53.4 \pm 2.1)^{+1.5}_{-1.9}$
MMHT2014nnlo68cl	$(47.7 \pm 5.1)^{+0.6}_{-0.8}$	$(52.3 \pm 2.9)^{+0.7}_{-1.0}$	$(53.8 \pm 2.2)^{+0.7}_{-1.0}$
MSHT20nnlo_as118	$(47.4 \pm 5.1)^{+0.5}_{-0.6}$	$(52.0 \pm 2.9)^{+0.6}_{-0.6}$	$(53.4 \pm 2.1)^{+0.6}_{-0.6}$
NNPDF40_nnlo_as_0.01180	$(47.8 \pm 5.1)^{+0.3}_{-0.3}$	$(52.4 \pm 2.9)^{+0.3}_{-0.3}$	$(53.8 \pm 2.2)^{+0.3}_{-0.3}$
PDF4LHC21_40	$(47.6 \pm 5.1)^{+0.8}_{-0.8}$	$(52.3 \pm 2.9)^{+0.9}_{-0.9}$	$(53.7 \pm 2.2)^{+0.9}_{-0.9}$
MSHT20an3lo_as118	$(45.0 \pm 4.8)^{+0.8}_{-0.7}$	$(49.4 \pm 2.8)^{+0.9}_{-0.8}$	$(50.7 \pm 2.0)^{+0.9}_{-0.8}$

Table 1: Higgs cross-section along with the absolute error obtained from seven-point scale variation around $(\mu_R^c, \mu_F^c) = (1, 1)m_H$ as well as intrinsic PDF uncertainty using LHAPDF. $\sqrt{S} = 14$ TeV, α_S from LHAPDF (NNLO value).

- Das, Moch, Vogt, Phys.Lett.B 807 (2020) 135546:

- ▶ N4LOsv: soft virtual ggF corrections at 4 loops
- ▶ N3LO: effective theory for $m_t \gg m_H$
- ▶ N2LO: full theory for $m_H \lesssim m_t$
- apparent convergence of perturbative series
(further details and predictions with $\mu/2$ in BACKUP)
- N4LOsv estimates missing higher-order corrections: 2%
- Larger differences originate from PDF and α_S sets:
7% (1995) → 12% (2020) → **7% (2024)** (more in BACKUP)
- Expect smaller effect of NNLO→N3LO PDFs



Some reasons for difference vs. other global fits

• Heavy-flavor PDF evolution and heavy flavour scheme for DIS

Phys.Rev.D 102 (2020) 5, 054014

- ▶ fixed-flavour number scheme in ABMP fits is accurate to NNLO for light and heavy quark production (exact or to the best available approximation) and works very well for HERA kinematics
- ▶ CT, MSHT and NNPDF fits use different variable-flavour number schemes which miss some NNLO corrections for heavy quark production and have further theoretical uncertainties \Rightarrow very relevant for LHC phenomenology

• Higher-twist (HT) corrections for DIS

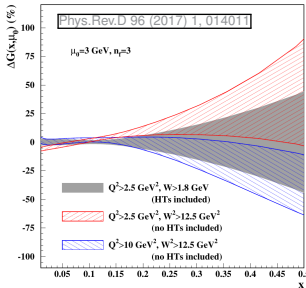
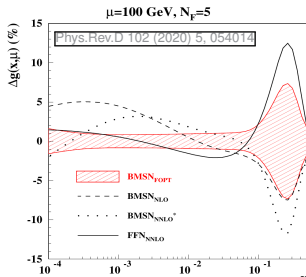
Phys.Rev.D 96 (2017) 1, 014011

- ▶ ABMPtt/ABMP16 fits HT terms
- ▶ other fits apply cuts to reduce HT: not sufficient

• Correlation between gluon PDF, α_S and m_t :

- ▶ fully accounted for in ABMPtt/ABMP16
- ▶ α_S and m_t are fixed in other fits

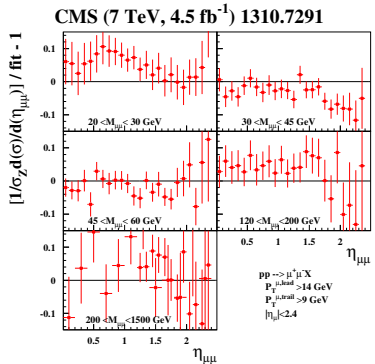
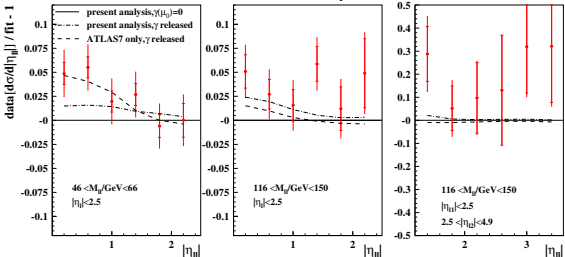
• These issues need to be solved independently of switching to N³LO evolution



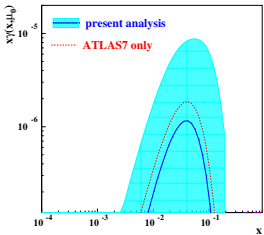
Photons in the proton and the new fit [preliminary ABMPgam]

- At increasingly higher orders, it is increasingly important to know the photon content of the proton and to include photon effects in PDF fits.
- Many PDF collaborations have already studied the role of the photon distribution in the proton. This has also been done in the case of the first aN3LO QCD PDF fits, see e.g.
[T. Cridge et al. \[arXiv:2312.07665\]](#).
- In the following we present work in progress in the ABMP framework, which will lead to the ABMPgam new fit. All results are preliminary and work is in progress.
- Two approaches have been considered so far:
 - (1) Photon according to the LUXqed approach
[A. Manohar et al. PRL 117 \(2016\) 242002](#), [A. Manohar et al. JHEP 12 \(2017\) 046](#)
 - implemented in most modern PDF fits (CT, MSHT, NNPDF), basically following the guidelines in the LUXqed papers, with some variations.
 - (2) Photon treated similarly to partons
 - photon distribution parameterized at a low scale and then evolved
 - initial condition fixed at such a scale (difficult to establish, because the available experimental data are hardly constraining photons at low scales).
 - photon evolves with standard evolution equations (resummation effects included)
 - approach used in “old” PDFs (i.e. PDF fits before the LUXqed approach was introduced) and by the ABMP collaboration in its new fit ABMPgam
- Selected preliminary results: effects of ATLAS and CMS dilepton data in shaping the initial condition for the photon distribution are presented in the following.

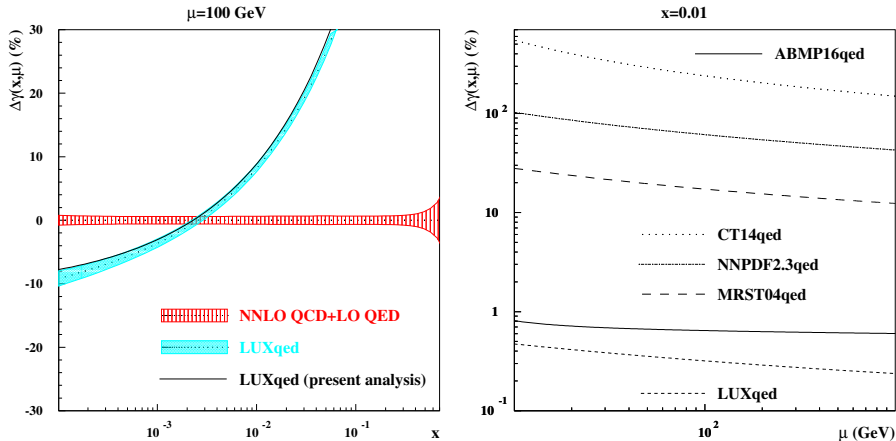
ABMPgam vs ATLAS and CMS data [preliminary]



- $\gamma\gamma \rightarrow \ell^+ \ell^-$ process at LO (FEWZ) included in the theory predictions compared to the data
- ATLAS data [ATLAS 1612.03016] at low ($M_{\ell^+ \ell^-}$, $y_{\ell^+ \ell^-}$) are in better agreement with central predictions obtained by assuming the presence of a photon component already at the initial starting scale μ_0 , but compatible with central predictions with $\gamma(\mu_0) = 0$ within $\sim 2.3\sigma$; other ATLAS data (backup) does not confirm this
- CMS data are consistent with initial condition $\gamma(\mu_0) = 0$, i.e. a photon generated purely perturbatively via evolution

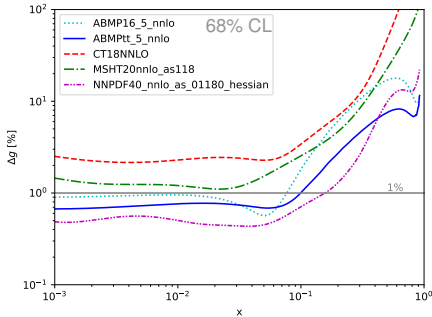
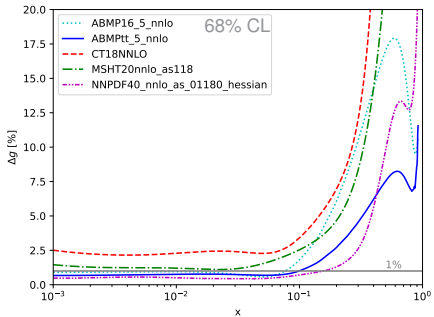


Fitted photon distribution [preliminary]



- Fixed $\gamma(\mu_0) = 0$, $\mu_0 = 3 \text{ GeV}$: consistent with data
- We find some difference w.r.t the LUXqed approach
 - ▶ ‘LUXqed (present analysis)’ refers to the LUXqed methodology on top of ABMP16
- Large spread of uncertainties on $\gamma(\mu, x)$
- This analysis should be repeated adding other data (e.g. the 13 TeV ones), including LHCb

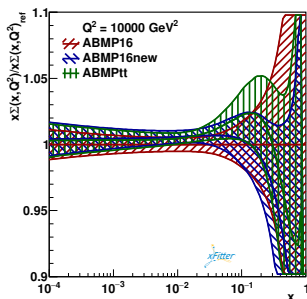
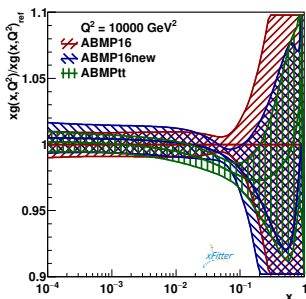
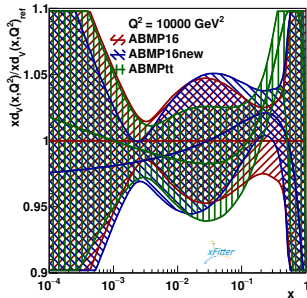
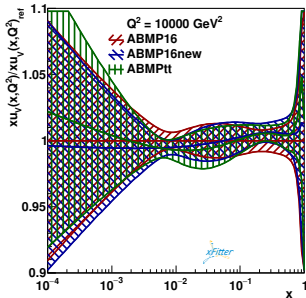
Summary and outlook



- ABMPtt NNLO fit includes new data on differential $t\bar{t}$, total $t\bar{t}$ and single t production
- PDFs, α_S and $m_t(m_t)$ are consistent with ABMP16 NNLO
- Uncertainty on gluon PDF reduced by up to a factor of 2 w.r.t ABMP16
- $\alpha_S(M_Z) = 0.1150 \pm 0.0009$ remains almost unchanged, but less correlated with $m_t(m_t)$
- ABMPtt done at exact NNLO for $t\bar{t}$ (no K factors etc.)
- ABMPtt gluon at large x is different vs. other global fits
 - ▶ important for LHC phenomenology, e.g. Higgs x-sections
- More information in [arXiv:2407.00545](https://arxiv.org/abs/2407.00545); LHAPDF tables will appear soon (ABMPtt_5_nnlo, ABMPtt_4_nnlo, ABMPtt_3_nnlo)
- Work in progress on fitting photon PDF in the proton

BACKUP

ABMPtt vs ABMP16



Data in ABMP16 fit [Alekhin et al., arXiv:1701:05838] (1)

Experiment	Process	Reference	NDP	χ^2
DIS				
HERA I+II	$e^\pm p \rightarrow e^\pm X$ $e^\pm p \rightarrow (\gamma)^\pm X$	[4]	1168	1510
BCDMS	$\mu^\pm p \rightarrow \mu^\pm X$	[61]	351	411
NMC	$\mu^\pm p \rightarrow \mu^\pm X$	[60]	245	343
SLAC-49a	$e^- p \rightarrow e^- X$	[54][62]	38	59
SLAC-49b	$e^- p \rightarrow e^- X$	[54][62]	154	171
SLAC-87	$e^- p \rightarrow e^- X$	[54][62]	109	103
SLAC-89b	$e^- p \rightarrow e^- X$	[56][62]	90	79

DIS heavy-quark production

HERA I+II	$e^\pm p \rightarrow e^\pm cX$	[63]	52	62
H1	$e^\pm p \rightarrow e^\pm bX$	[15]	12	5
ZEUS	$e^\pm p \rightarrow e^\pm bX$	[16]	17	16
CCFR	$(\gamma)^\pm p \rightarrow \mu^\pm cX$	[64]	89	62
CHORUS	$\nu p \rightarrow \mu^\pm cX$	[18]	6	7.6
NOMAD	$\nu p \rightarrow \mu^\pm cX$	[17]	48	59
NuTeV	$(\gamma)^\pm \nu \rightarrow \mu^\pm cX$	[64]	89	49

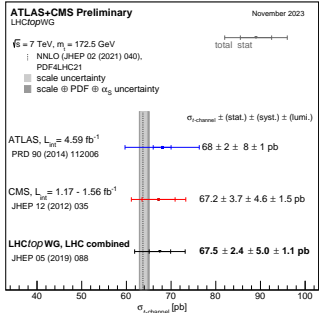
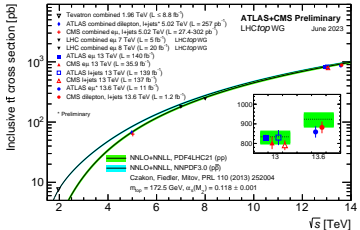
DY

FNAL-605	$pCu \rightarrow \mu^+ \mu^- X$	[67]	119	165
FNAL-866	$pp \rightarrow \mu^+ \mu^- X$ $pD \rightarrow \mu^+ \mu^- X$	[68]	39	53

Top-quark production

ATLAS, CMS	$pp \rightarrow tqX$	[27][52]	10	2.3
CDF&DØ	$\bar{p}p \rightarrow tbX$ $\bar{p}p \rightarrow tqX$	[53]	2	1.1
ATLAS, CMS	$pp \rightarrow t\bar{t}X$	[33][52]	23	13
CDF&DØ	$\bar{p}p \rightarrow t\bar{t}X$	[53]	1	0.2

$t\bar{t}$ and single top LHC data have been updated to latest LHCTOPWG:



Data in ABMP16 fit [Alekhin et al., arXiv:1701:05838] (2)

Experiment	ATLAS		CMS		DØ		LHCb			
\sqrt{s} (TeV)	7	13	7	8	1.96		7	8		
Final states	$W^+ \rightarrow l^+ \nu$	$W^+ \rightarrow l^+ \nu$	$W^+ \rightarrow \mu^+ \nu$	$W^+ \rightarrow \mu^+ \nu$	$W^+ \rightarrow \mu^+ \nu$	$W^+ \rightarrow e^+ \nu$	$W^+ \rightarrow \mu^+ \nu$	$Z \rightarrow e^+ e^-$	$W^+ \rightarrow \mu^+ \nu$	
	$W^- \rightarrow l^- \nu$	$W^- \rightarrow l^- \nu$	$W^- \rightarrow \mu^- \nu$	$W^- \rightarrow \mu^- \nu$	$W^- \rightarrow \mu^- \nu$	$W^- \rightarrow e^- \nu$	$W^- \rightarrow \mu^- \nu$	$W^- \rightarrow \mu^- \nu$	$Z \rightarrow \mu^+ \mu^-$	
	$Z \rightarrow l^+ l^-$	$Z \rightarrow l^+ l^-$	(asym)		(asym)					
Cut on the lepton P_T	$P_T^l > 20$ GeV	$P_T^e > 25$ GeV	$P_T^\mu > 25$ GeV	$P_T^\mu > 25$ GeV	$P_T^\mu > 25$ GeV	$P_T^e > 25$ GeV	$P_T^\mu > 20$ GeV	$P_T^e > 20$ GeV	$P_T^\mu > 20$ GeV	
Luminosity (fb $^{-1}$)	0.035	0.081	4.7	18.8	7.3	9.7	1	2	2.9	
Reference	[66]	[26]	[24]	[25]	[23]	[22]	[19]	[21]	[20]	
NDP	30	6	11	22	10	13	31	17	32	
χ^2	present analysis ^a	31.0	9.2	22.4	16.5	17.6	19.0	45.1	21.7	40.0
	CJ15 [6]	–	–	–	–	20	29	–	–	–
	CT14 [7]	42	–	– ^b	–	–	34.7	–	–	–
	JR14 [8]	–	–	–	–	–	–	–	–	–
	HERAFitter [197]	–	–	–	–	13	19	–	–	–
	MMHT14 [9]	39	–	–	–	21	–	–	–	–
	NNPDF3.0 [10]	35.4	–	18.9	–	–	–	–	–	–

^a The ABM12 [1] analysis has used older data sets from CMS and LHCb.

^b For the statistically less significant data with the cut of $P_T^\mu > 35$ GeV the value of $\chi^2 = 12.1$ was obtained.

TABLE VI: Compilation of precise data on W - and Z -boson production in pp and $p\bar{p}$ collisions and the χ^2 values obtained for these data sets in different PDF analyses using their individual definitions of χ^2 . The NNLO fit results are quoted as a default, while the NLO values are given for the CJ15 [6] and HERAFitter [197] PDFs. Missing table entries indicate that the respective data sets have not been used in the analysis.

Experiment	Data set	\sqrt{s} (TeV)	Reference	NDP	χ^2		
					I	II	III
ATLAS	$ATLAS\,13_{ljet}$	13	[25]	19	34.2	27.2	–
	$ATLAS\,13_{had}$	13	[26]	10	11.8	12.1	–
CMS	$CMS\,13_{ll}$	13	[24]	15	21.1	–	19.9
	$CMS\,13_{ljet}$	13	[22]	34	42.2	–	40.8

I: both ATLAS and CMS

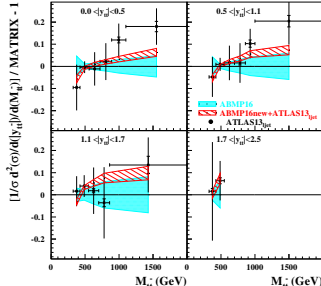
II: only ATLAS

III: only CMS

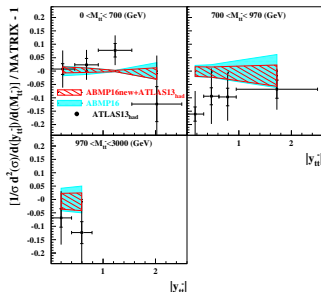
→ Overall good description of data by NNLO theoretical predictions, but some tension between ATLAS and CMS differential $t\bar{t}$ data is noticeable

Other $t\bar{t}$ differential data in ABMP16 PDF fit

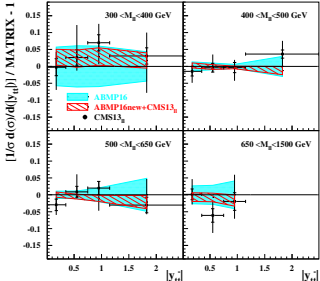
ATLAS ($\sqrt{s}=13$ TeV, 36 fb^{-1} , $\text{pp} \rightarrow t\bar{t}X \rightarrow \text{ljet}X$) 1908.07305



ATLAS ($\sqrt{s}=13$ TeV, 36 fb^{-1} , $\text{pp} \rightarrow t\bar{t}X \rightarrow \text{hadrons}X$) 2006.09274

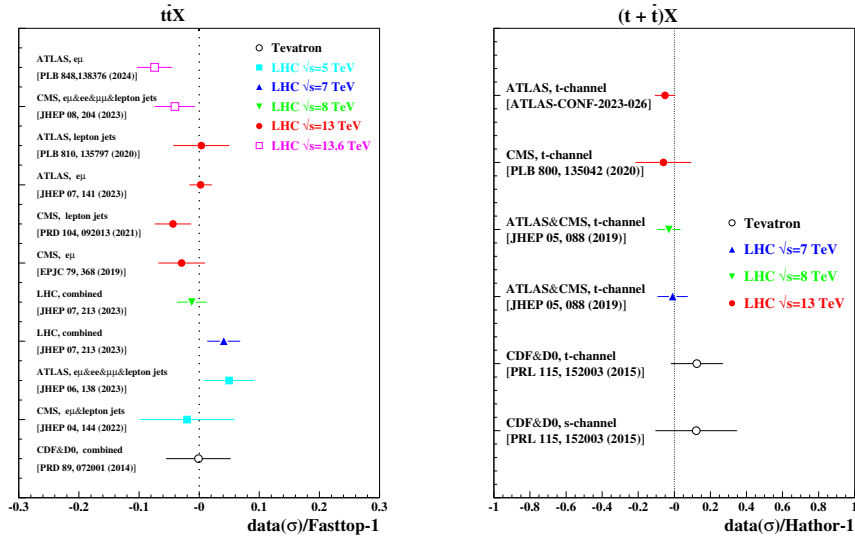


CMS ($\sqrt{s}=13$ TeV, 36 fb^{-1} , $\text{pp} \rightarrow t\bar{t}X \rightarrow t^{\prime}\bar{t}'X$) 1904.05237



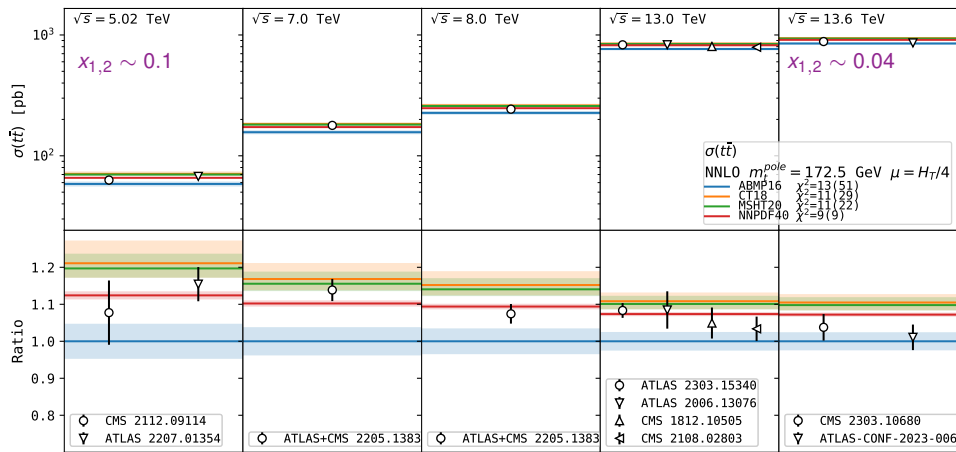
→ all data are in good agreement with NNLO theoretical predictions and put significant constraints on the PDFs

$\sigma(t\bar{t})$ and single t in ABMP16 PDF fit



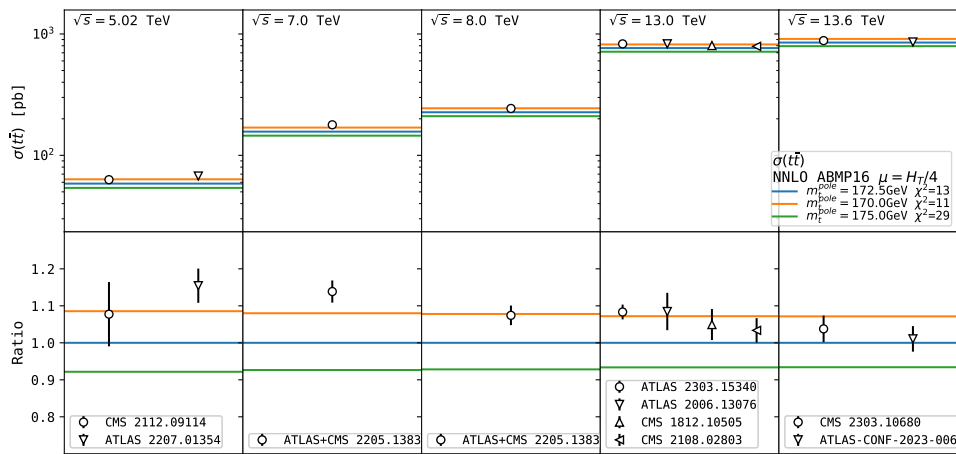
- good description of total $t\bar{t}$ and single t data
- single t data provide additional constraint on m_t (less correlated with g and α_S)

$\sigma(t\bar{t})$ vs NNLO predictions using different PDFs



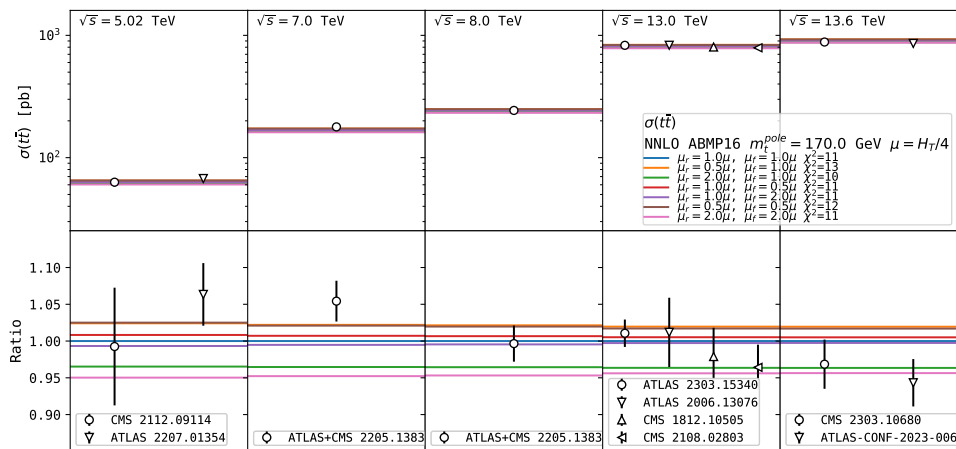
- Fixed $m_t^{\text{pole}} = 172.5 \text{ GeV}$, $\mu_r = \mu_f = H_T/4$
- Reported χ^2 values with (and without) PDF uncertainties
- All PDF sets describe data reasonably well (depends on m_t^{pole} , α_S)
- Sensitivity to PDFs reduces with increasing \sqrt{s} (lower x probed)

$\sigma(t\bar{t})$ vs NNLO predictions using different m_t^{pole}



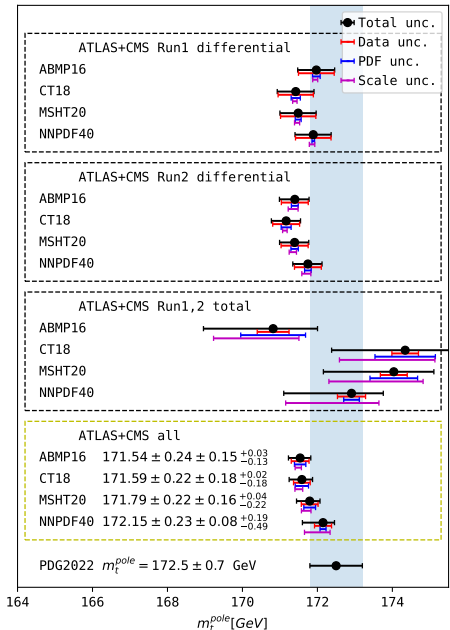
- ABMP16, fixed $\mu_r = \mu_f = H_T/4$
- Change of m_t^{pole} by 1 GeV \rightarrow change of $\sigma(t\bar{t})$ by $\approx 3\%$
- Preferable $m_t^{\text{pole}} \sim 170\text{--}172.5 \text{ GeV}$ (depends on PDF and α_S)

$\sigma(t\bar{t})$ vs NNLO predictions with scale variations



- ABMP16, fixed $m_t^{\text{pole}} = 172.5$ GeV
- Scale variations $\pm 3\%$:
 - ▶ larger than data uncertainty (best data uncertainty $\pm 1.9\%$)
 - ▶ limit precision of m_t^{pole} extraction to 1 GeV
 - ▶ can be reduced by using e.g. $\overline{\text{MS}}$ mass $m_t(m_t)$ EPJ C74 (2014) 3167, JHEP04 (2021) 043

Extraction of m_t^{pole} : summary

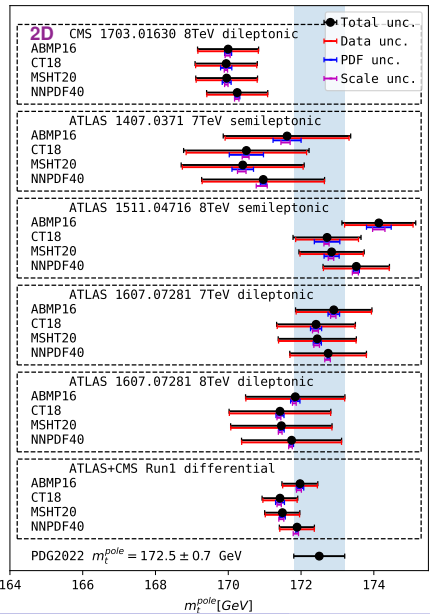


- Extracted m_t^{pole} values with precision $\pm 0.3 \text{ GeV}$ are consistent with PDG value $172.5 \pm 0.7 \text{ GeV}$
 - data uncertainty $\sim 0.2 \text{ GeV}$
 - PDF uncertainty $\sim 0.1 \text{ GeV}$
 - NNLO scale uncertainty $\sim 0.2 \text{ GeV}$
- Significant dependence on PDFs ($\sim 0.5 \text{ GeV}$)
 - different m_t^{pole} used in different PDFs
 - PDFs, m_t^{pole} , α_s should be determined simultaneously
- For CMS 1904.05237, NNLO results are consistent with published results obtained at NLO
 - good convergence of perturbative series
- Larger sensitivity comes from differential data
 - 2D differential x-sections in $M(t\bar{t})$, $y(t\bar{t})$ constrain m_t^{pole} , PDFs and (indirectly) α_s
 - ideally, 3D cross section in $M(t\bar{t})$, $y(t\bar{t})$ and number of extra jets constrain α_s directly, but NNLO not yet available for $t\bar{t} + \text{jets}$
- Possible effects from Coulomb and soft-gluon resummation near the $t\bar{t}$ production threshold are neglected: might be $\sim 1 \text{ GeV}$

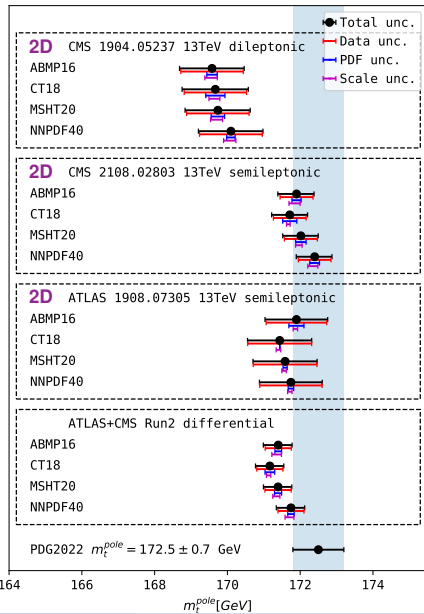
[CMS Coll. EPJ C80 (2020) 658; Kiyo, Kuhn, Moch, Steinhauser, Uwe EPJ C60 (2009) 375; Mäkelä, Hoang, Lipka, Moch 2301.03546]

Extraction of m_t^{pole} : differential Run 1, Run 2

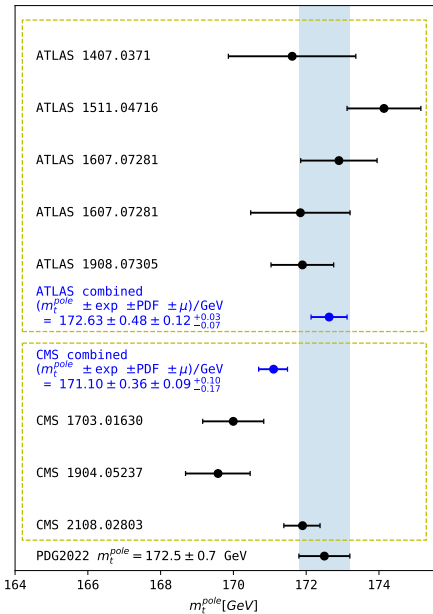
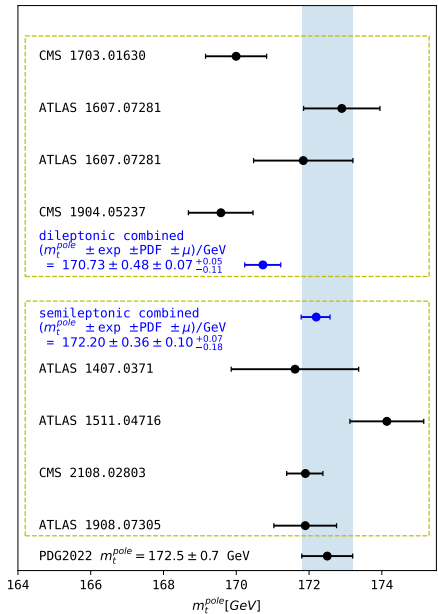
Run 1 differential



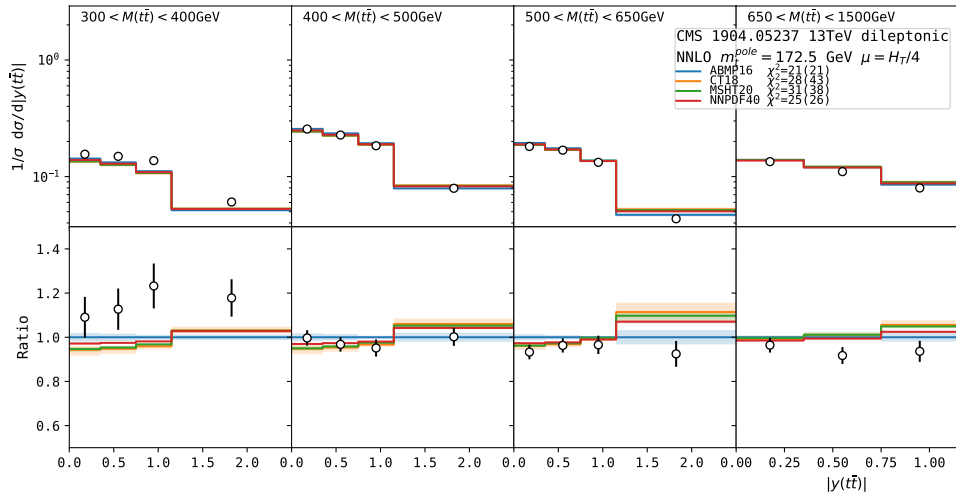
Run 2 differential



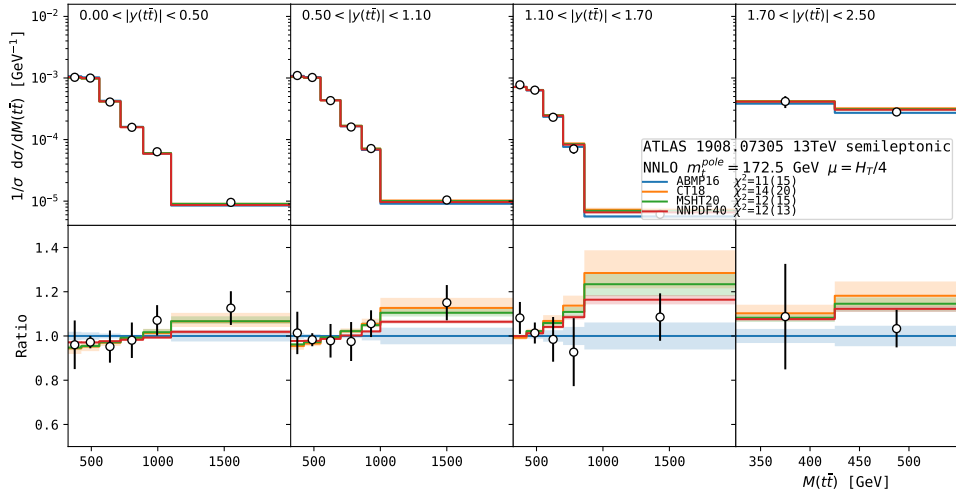
Extraction of m_t^{pole} : dilepton vs semileptonic, ATLAS vs CMS



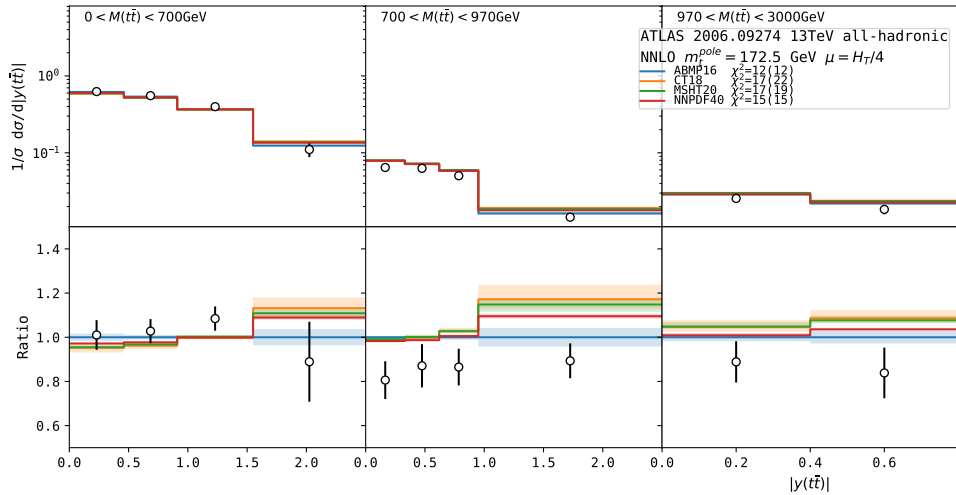
Data vs NNLO predictions using different PDFs



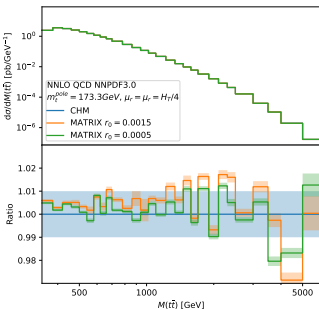
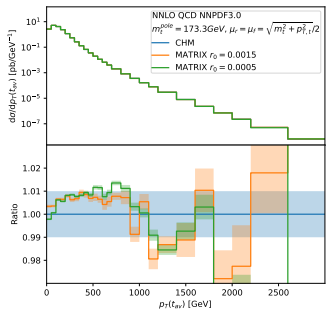
Data vs NNLO predictions using different PDFs



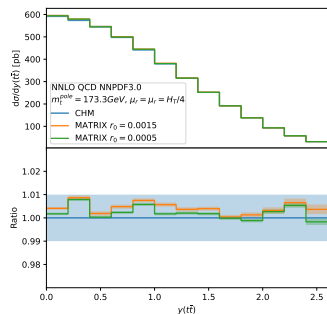
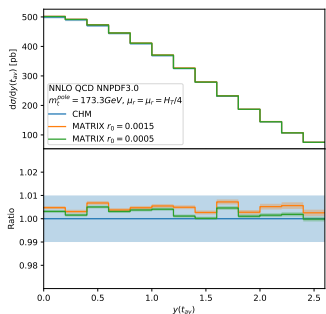
Data vs NNLO predictions using different PDFs



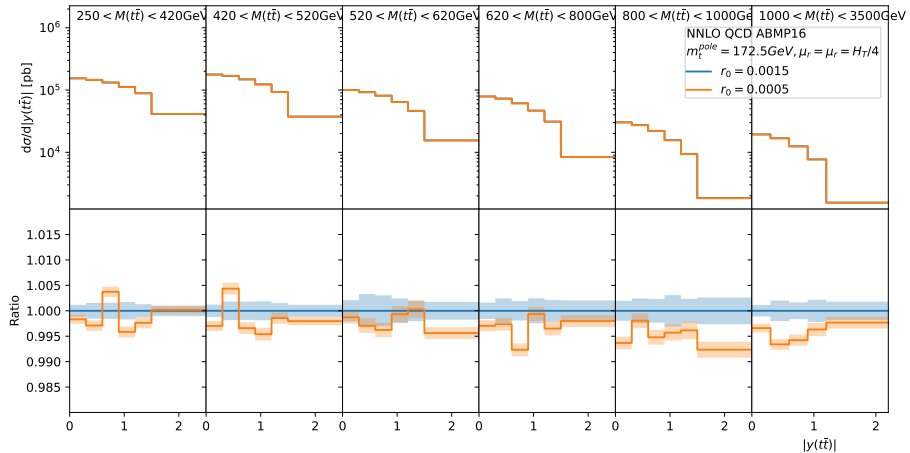
Variation of r cut, validation vs JHEP 04 (2017) 071 by Czakon et al. [CHM]



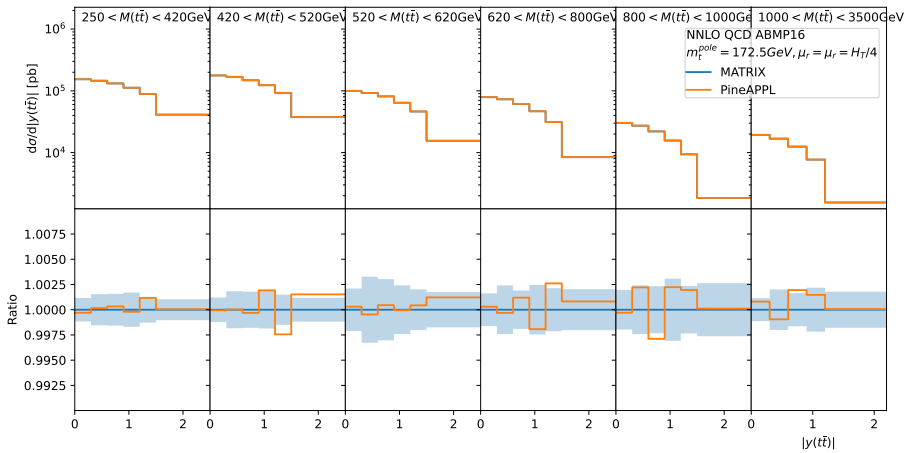
Good agreement < 1%



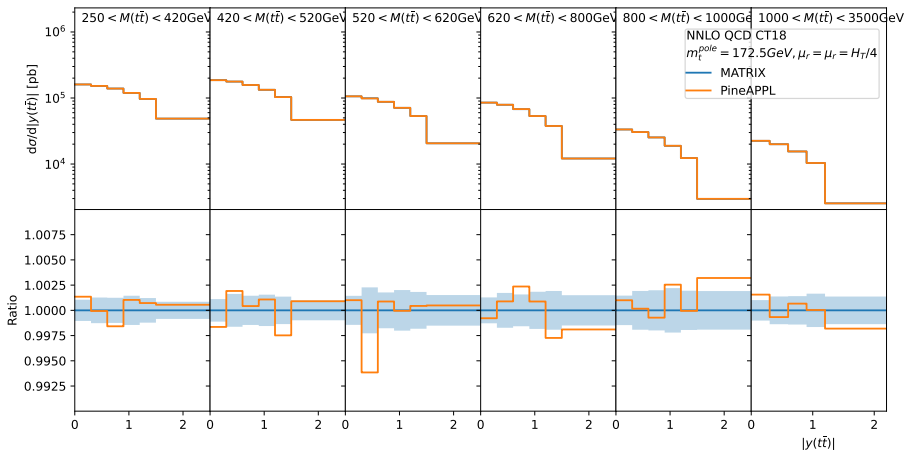
r cut variation in bins of TOP-20-001



PineAppl vs MATRIX in bins of TOP-20-001 [ABMP16]

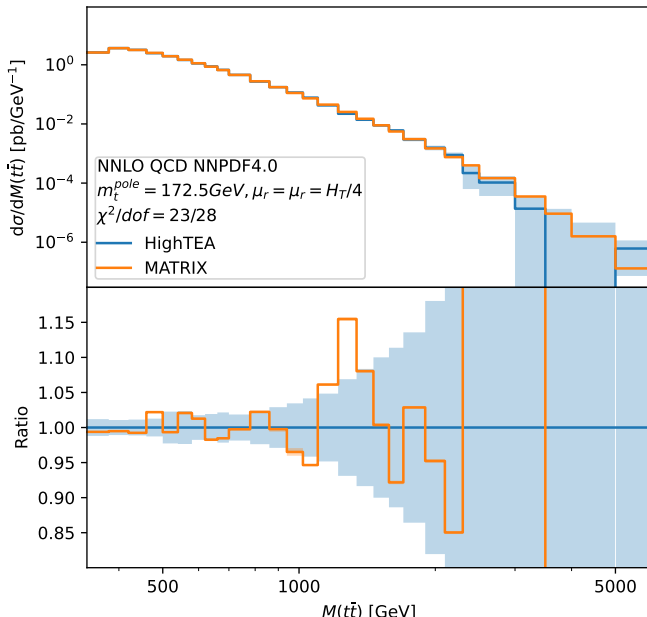


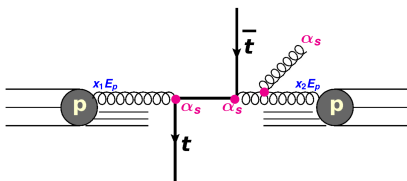
PineAppl vs MATRIX in bins of TOP-20-001 [CT18]



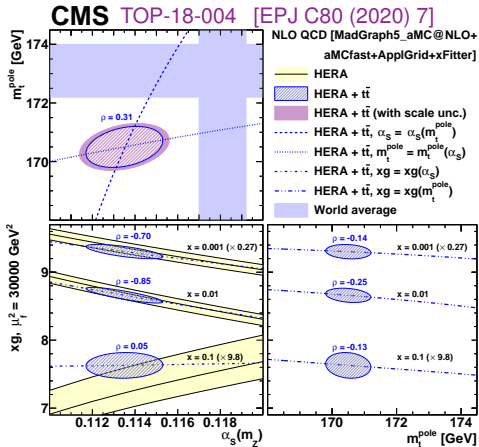
- grids were produced with ABMP16

MATRIX vs HighTEA



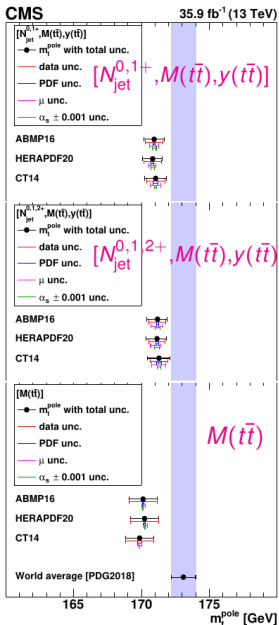
Example:Why study $t\bar{t}$ production?

- m_t provides a hard scale
⇒ ultimate probe of pQCD
(NLO, aNNLO, NNLO, ...)
- Produced mainly via gg
⇒ constrain gluon PDF at high x
- Production sensitive to α_s and m_t^{pole}
- May provide insight into possible new physics

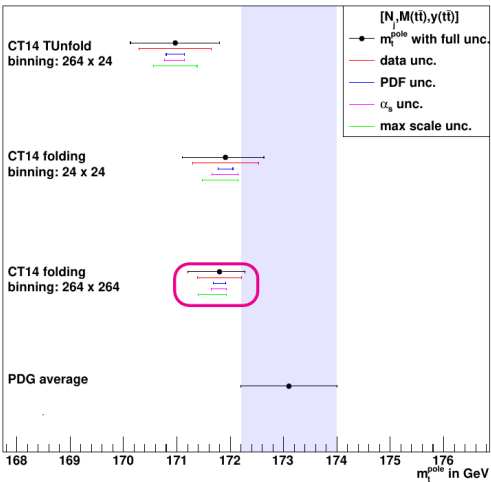


- Simultaneous extraction of PDFs, α_s , m_t^{pole} using normalised triple-differential cross sections at NLO
- Extended to $\overline{\text{MS}}$, MSR schemes in JHEP 04 (2021) 043 [Garzelli, Kemmler, Moch, Zenaiev]

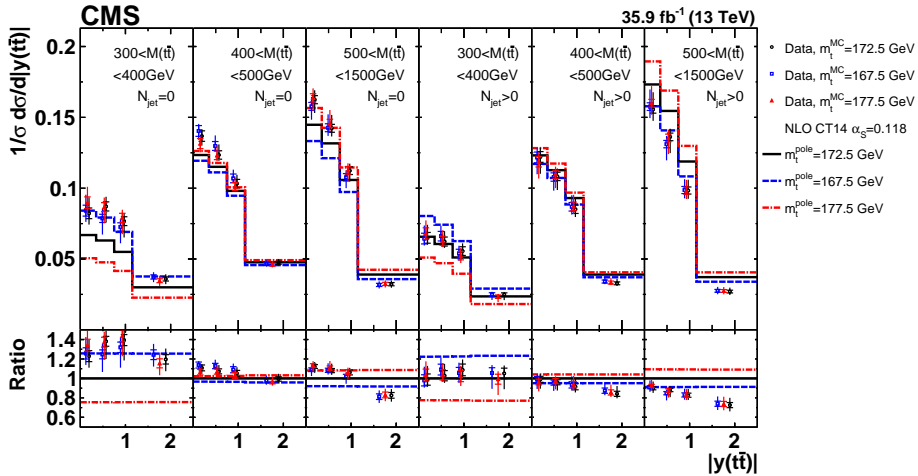
CMS TOP-18-004 checks



DESY 2018 summer school, L. Materne, bachelor thesis
 "Differential Top-Pair Production Cross Section with the CMS Detector - Optimization of Measurement Information",
 Karlsruher Institut für Technologie (KIT), Bachelorarbeit,
 2018 [ETP-Bachelor-KA/2018-11]

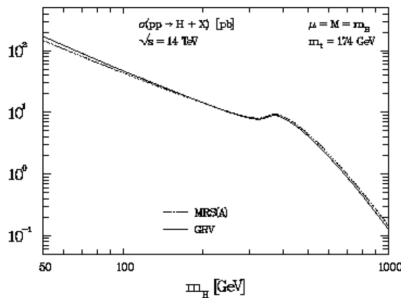


m_t dependence of measured cross sections [CMS TOP-18-004]



Higgs cross section (1995)

NLO QCD corrections



MRS(A): Martin, Roberts and Stirling,
Phys. Rev. D50 (1994) 6734

GRV: Glück, Reya and Vogt,
Z. Phys. C53 (1992) 127

One of the main uncertainties in the prediction of the Higgs production cross section is due to the gluon density. [...] Adopting a set of representative parton distributions [...], we find a variation of about 7% between the maximum and minimum values of the cross section for Higgs masses above $\sim 100 \text{ GeV}$.

Spira, Djouadi, Graudenz, Zerwas (1995)
hep-ph/9504378

Higgs cross section (2020)

- Cross section $\sigma(H)$ at NNLO with uncertainties: $\sigma(H) + \Delta\sigma(\text{PDF} + \alpha_s)$ for $m_H = 125.0 \text{ GeV}$ at $\sqrt{s} = 13 \text{ TeV}$ with $\mu_R, \mu_F = m_H$ and nominal α_s

PDF sets	$\sigma(H)^{\text{NNLO}} [\text{pb}]$ nominal $\alpha_s(M_Z)$
ABMP16 Alekhin, Blümlein, S.M., Placakyte '17	40.20 ± 0.63
CJ15 Accardi, Brady, Melnitchouk et al. '16	$42.45^{+1.73}_{-1.12}$
CT18 Hou et al. '19	$42.06^{+1.16}_{-1.48}$
HERAPDF2.0 H1+Zeus Coll.	$42.62^{+0.35}_{-0.43}$
JR14 (dyn) Jimenez-Delgado, Reya '14	38.01 ± 0.34
MMHT14 Martin, Motylinski, Harland-Lang, Thorne '14	$42.36^{+0.56}_{-0.78}$
NNPDF3.1 Ball et al. '17	42.98 ± 0.40
PDF4LHC15 Butterworth et al. '15	42.42 ± 0.78

- Large spread for predictions from different PDFs $\sigma(H) = 38.0 \dots 43.0 \text{ pb}$
- PDF and α_s differences between sets amount to up to 12%
 - significantly larger than residual theory uncertainty due to N³LO QCD and NLO electroweak corrections

Higgs cross section with $\mu/2$

PDF Name	N2LO	N3LO	N4LOsv
ABMP16	$(49.9 \pm 4.6)^{+0.8}_{-0.8}$	$(51.2 \pm 1.6)^{+0.9}_{-0.9}$	$(51.3 \pm 1.7)^{+0.9}_{-0.9}$
ABMPtt	$(49.6 \pm 4.6)^{+0.7}_{-0.7}$	$(50.8 \pm 1.6)^{+0.8}_{-0.8}$	$(50.9 \pm 1.7)^{+0.8}_{-0.8}$
CT18NNLO	$(52.3 \pm 5.1)^{+1.4}_{-1.9}$	$(53.8 \pm 1.9)^{+1.5}_{-2.0}$	$(53.9 \pm 2.0)^{+1.5}_{-2.0}$
MMHT2014nnlo68cl	$(52.8 \pm 5.1)^{+0.7}_{-1.0}$	$(54.2 \pm 1.9)^{+0.7}_{-1.0}$	$(54.3 \pm 2.1)^{+0.7}_{-1.0}$
MSHT20nnlo_as118	$(52.5 \pm 5.1)^{+0.6}_{-0.6}$	$(53.9 \pm 1.9)^{+0.6}_{-0.7}$	$(54.0 \pm 2.1)^{+0.6}_{-0.7}$
NNPDF40_nnlo_as_01180	$(52.9 \pm 5.1)^{+0.3}_{-0.3}$	$(54.3 \pm 1.9)^{+0.3}_{-0.3}$	$(54.4 \pm 2.1)^{+0.3}_{-0.3}$
PDF4LHC21_40	$(52.7 \pm 5.1)^{+0.9}_{-0.9}$	$(54.1 \pm 1.9)^{+0.9}_{-0.9}$	$(54.2 \pm 2.1)^{+0.9}_{-0.9}$
MSHT20an3lo_as118	$(49.3 \pm 4.8)^{+0.9}_{-0.8}$	$(51.1 \pm 1.8)^{+1.0}_{-0.8}$	$(51.2 \pm 2.0)^{+1.0}_{-0.9}$

Table 2: Higgs cross-section along with the absolute error obtained from seven-point scale variation around $(\mu_R^c, \mu_F^c) = (1/2, 1)m_H$ as well as intrinsic PDF uncertainty using LHAPDF. $\sqrt{S} = 14$ TeV, α_S from LHAPDF (NNLO value).

Higgs cross section details [Goutam Das]

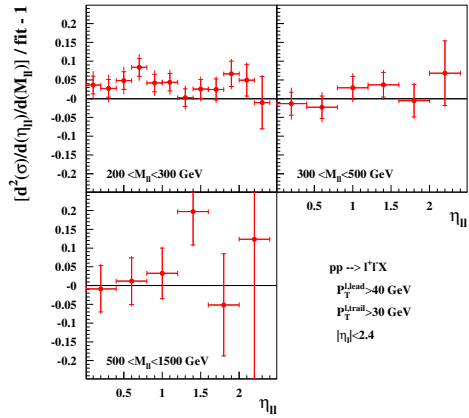
We keep the setting same as the Higgs paper: $\kappa_4 = 1/25000 \simeq 1/(4\pi)^4$, $\kappa_4 g_{0,4} = 65 \pm 65$.

The predictions for the ggF cross sections at the collision energy of 14 TeV use a Higgs mass $m_H = 125$ GeV, an on-shell top quark mass $m_t = 172.5$ GeV, $n_f = 5$ active quark flavors and the PDF sets ABMP16 [?] and MMHT2014 [?] using the `1hapdf` [?] interface. The PDF sets and as well as the value of the strong coupling constant α_s corresponding to the respective PDF set are taken order-independent at NNLO throughout. The prefactor $C(\mu_R^2)$ in Eq. (??) is improved with the full top-mass dependence of the Born cross section. The results up to N³LO are computed with the program *iHixs* [?] which directly provides the cross sections in this rescaled effective field theory.

The central scale choices $\mu_R^c = \mu_F^c = m_H$ and $\mu_R^c = m_H/2, \mu_F^c = m_H$. For $\sqrt{S} = 14$ TeV, $m_H^c = 125$ GeV, the central scale $\mu_R = m_H$, and including the PDF uncertainties at N³LO.

ABMPgam vs ATLAS data [preliminary]

ATLAS (8 TeV, 20.3 fb^{-1}) 1606.01736



ATLAS (8 TeV, 20.2 fb^{-1}) 1710.05167

